A R C H I V E O F M E C H A N I C A L E N G I N E E R I N G

VOL. LXV 2018 Number 1

DOI: 10.24425/119409

Key words: microbeams, temperature-dependent properties, modified couple stress analysis, linear varying thickness

ASHRAF M. ZENKOUR[1, 2]

MODIFIED COUPLE STRESS THEORY FOR MICRO-MACHINED BEAM RESONATORS WITH LINEARLY VARYING THICKNESS AND VARIOUS BOUNDARY CONDITIONS

This article employs the classical Euler–Bernoulli beam theory in connection with Green–Naghdi's generalized thermoelasticity theory without energy dissipation to investigate the vibrating microbeam. The microbeam is considered with linearly varying thickness and subjected to various boundary conditions. The heat and motion equations are obtained using the modified couple stress analysis in terms of deflection with only one material length-scale parameter to capture the size-dependent behavior. Various combinations of free, simply-supported, and clamped boundary conditions are presented. The effect of length-to-thickness ratio, as well as the influence of both couple stress parameter and thermoelastic coupling, are all discussed. Furthermore, the effect of reference temperature on the eigenfrequency is also investigated. The vibration frequencies indicate that the tapered microbeam modeled by modified couple stress analysis causes more responses than that modeled by classical continuum beam theory, even the thermoelastic coupled is taken into account.

1. Introduction

The classical couple stress analyses have been developed to describe size-dependent effects [1–4]. In fact, the couple-stresses concept in continuum mechanics is receiving greater attention by many researchers owing to its theoretical and practical interest. Cosserat and Cosserat [1] have been considered as the first researchers who developed a mathematical model to analyze materials with couple stresses. The couple-stress analysis is an extended form of the continuum theory that includes effects of a couple and shear forces per unit area. Later on, Toupin [2]

[1] *Department of Mathematics, Faculty of Science, King Abdulaziz University, P.O. Box 80203, Jeddah 21589, Saudi Arabia. Email: zenkour@kau.edu.sa*

[2] *Department of Mathematics, Faculty of Science, Kafrelsheikh University, Kafrelsheikh 33516, Egypt. Email: .Email: zenkour@sci.kfs.edu.eg*

has derived the associative constitutive equations for finite deformation of perfectly elastic materials and Mindlin and Tiersten [3] have formulated a literalized theory of couple stress elasticity. So, a couple stress analysis, using macro-rotation as true kinematical rotation, has been discussed by Toupin [2], Mindlin and Tiersten [3], Koiter [4], and others for different elastic continuums. Tiwari [5] has used Cosserats equations [1, 3] to deduce the effect of couple stress on deflection produced in a semi-infinite elastic body due to impulsive twist over bounding surface.

It is assumed, in linearized couple-stress analysis, that the couple-stresses are proportional to the curvature, and a new material coefficient ϑ is introduced with a dimension of length. Braun [6] has reformulated the linear couple-stress analysis of Mindlin and Tiersten [3] to provide a systematic compilation of governing differential equations. Yang et al. [7] have formed a modified couple stress theory by reducing two higher-order material length-scale parameters to only one. The purpose of this feature is to make modified couple stress analysis easier for many applications. Recently, the modified couple stress analyses have been developed and extensively used in many aspects to discuss the mechanical behavior of microstructures.

In fact, the modified couple stress theory that developed by Yang et al. [7] with one internal length-scale parameter has been widely attracted interest. Park and Gao [8, 9] have developed new model for bending of Euler–Bernoulli beam and presented variational formulation by using modified couple stress analysis. Ma et al. [10, 11] have studied microstructure-dependent Timoshenko's beam theory and non-classical Mindlin plate theory using modified couple stress analysis. Tsiatas [12] and Yin et al. [13] have developed a Kirchhoff's plate theory with modified couple stress analysis for static and dynamic analyses of isotropic microscale plates with arbitrary shapes. Fu and Zhang [14] have established a Timoshenko's beam model to study the size-effects of microtubules via the modified couple stress analysis. Güven [15] has discussed the propagation of longitudinal stress waves based on a Love rod theory taking into account the effects of lateral deformation. Reddy and Arbind [16] have reformulated Euler–Bernoulli's and Timoshenko's beam models using modified couple stress analysis for microstructure-dependent functionally graded (FG) beams. Chen and Li [17] have developed a micro-scale free vibration behavior of composite laminated Timoshenko's beam theory based on the new modified couple stress analysis. Gao et al. [18] have developed non-classical third-order shear deformation plate theory using modified couple stress analysis and variational formulation. Wang et al. [19] have proposed non-classical Kirchhoff's plate theory for axisymmetrically nonlinear bending analysis of circular microplates subjected to uniform load based on modified couple stress analysis. Chen and Li [20] have proposed new modified couple stress analysis that containing three material length-scale parameters for anisotropic elasticity.

Recently, Darijani and Shahdadi [21] have proposed a new 2-unknown shear deformation plate theory for static and dynamic analyses of microplates using modified couple stress analysis. Zeighampour and Beni [22] have obtained the formulation of thin cylindrical shell based on modified couple stress analysis by taking into account the effect of shear deformation and rotary inertia. Setoodeh et al. [23] have analytically investigated the linear and nonlinear torsional free vibration analyses of FG micro/nano-tubes based upon modified couple stress analysis. Sourki and Hoseini [24] have investigated free vibration behavior of cracked microbeam based on modified couple stress analysis using Euler–Bernoulli's beam theory. Additional researchers have performed their investigations on static and dynamic behavior of microstructures based on modified couple stress analysis [25–38].

Nowacki [39] has presented some generalized theorems on the coupled thermoelasticity of a medium characterized by the displacement and rotation as independent vectors. He has derived the constitutive equations and the expanded equation of heat conductivity for an isotropic medium based on the couple stress theory. Rezazadeh et al. [40] have studied some expressions for quality factor of thermoelastic damping with the application of modified couple stress analysis for plane stress and strain conditions. Taati et al. [41] have derived size-dependent, explicit formulation for coupled thermoelasticity to address Timoshenko's microbeam behavior. They have combined the modified couple stresses and non-Fourier heat conduction to capture size-effects in the microscale. Kumar et al. [42] have dealt with the plane wave propagations in homogeneous isotropic couple stress generalized thermoelastic medium. Zhong et al. [43] have investigated size-dependent thermoelastic damping in microplate resonators based upon modified couple stress analysis. Kumar [44] has investigated equations of motion for modified couple stress theory and heat conduction equation for coupled thermoelasticity are investigated to model vibrations in homogeneous thin beam in a closed-form by applying Euler–Bernoulli's beam theory.

In this study, vibrational frequency analysis of a tapered microbeam resonator is investigated via a generalized thermoelastic theory in connection with modified couple stress analysis. The thickness is linearly varying and the microbeam material is assumed to be size-dependent according to modified couple stress analysis, and deformation is considered according the classical Euler–Bernoulli's beam theory. To study the effect of boundary conditions, four types of end conditions, i.e., clamped-clamped, supported-supported, clamped-supported and clamped-free, are considered. Governing differential equations of tapered microbeams are formulated. Several numerical results for tapered microbeams are graphically illustrated. Additional results are tabulated to discuss the size-dependent vibration behavior and the effect of the reference temperature.

2. Modified couple stress theory

A micro-machined beam with linear varying thickness [45–54] is considered here. It is chosen to be homogenous, isotropic and thermally conducting. Shown in Fig. 1 is the microbeam having dimensions of length L $(0 \leqslant x \leqslant L)$, width b $(-b/2 \leqslant y \leqslant +b/2)$ and varying thickness $(h/2)$ $(0 \leqslant z \leqslant +h/2)$ at $x = 0$, and h

$(-h/2 \leqslant z \leqslant +h/2)$ at $x = L$. The x-axis is taken along the axis of the microbeam, y-axis along the width, and z-axis along the thickness. The present microbeam is unstrained, unstressed, and also kept at a uniform reference temperature T_0 in the equilibrium case.

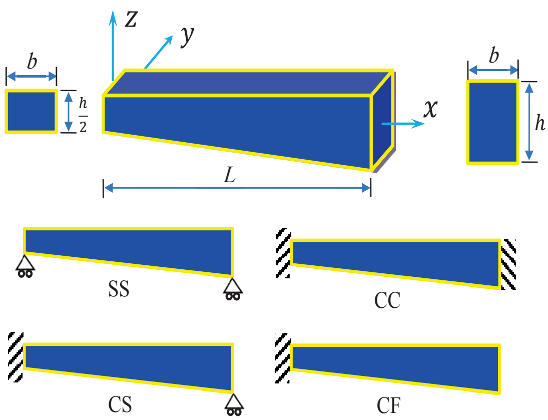

Fig. 1. Schematic diagram for the tapered micro-machined beam

Firstly, the following integral operator is appropriate to the present a tapered microbeam

$$\mathcal{L}_p(\cdot) = \int\limits_{-b/2}^{b/2} \left[\int\limits_{0}^{h/2} (\cdot) z^p \mathrm{d}z + \frac{1}{2} \int\limits_{-h/2}^{0} (\cdot) z^p \mathrm{d}z \right] \mathrm{d}y. \tag{1}$$

For example, the geometrical properties of tapered microbeam such as cross-section area (A) and second moment of cross-section area (I) can be considered, with the aid of Eq. (1), as

$$\{A, I\} = \{\mathcal{L}_0(1), \mathcal{L}_2(1)\} = \left\{ \frac{3}{4} bh,\ \frac{1}{16} bh^3 \right\}. \tag{2}$$

The classical thin beam linear Euler-Bernoulli theory is appropriate to deal with such tapered micro-machined beam. The displacements of such a theory are presented as

$$u_1(x, y, z, t) = u(x, z, t) = -z \frac{\partial w}{\partial x}, \qquad u_2 = 0, \qquad u_3(x, y, z, t) = w(x, t), \tag{3}$$

where u represents the axial displacement, w represents the transverse displacement (deflection) and t is the time. The constitutive relations for the present classical theory based upon the modified couple stress analysis will be reduced to

$$\begin{aligned} \sigma_x &= -(\lambda + 2\mu) z \frac{\partial^2 w}{\partial x^2} - \beta\theta, \\ m_{xy} &= -\mu\vartheta^2 \frac{\partial^2 w}{\partial x^2}, \end{aligned} \tag{4}$$

in which σ_x is the axial stress, m_{xy} is the in-plane couple stress, $\theta = T - T_0$ represents the excess temperature distribution, in which T_0 is the environment (reference) temperature and $T(x, z, t)$ is the temperature at any point; $\beta = (3\lambda + 2\mu)\alpha_t$ is the coupling parameter in which α_t denotes the coefficient of linear thermal expansion; λ and μ are Lamé's parameters, and ϑ denotes the couple stress (material length-scale) coefficient. The flexural moment of tapered microbeam can be illustrated as

$$M(x,t) = -\mathcal{L}_1(\sigma_x) - \mathcal{L}_0(m_{xy}). \tag{5}$$

With the aid of Eq. (4), one gets

$$M(x,t) = (\lambda + 2\mu) I \frac{\partial^2 w}{\partial x^2} + \beta M_T + \mu\vartheta^2 A \frac{\partial^2 w}{\partial x^2}. \tag{6}$$

Here M_T represents the thermal moment of the tapered microbeam and it is given by

$$M_T = \mathcal{L}_1(\theta(x, z, t)). \tag{7}$$

For transversely vibration of tapered microbeams, the equation of motion according to Euler–Bernoulli's theory is given by

$$\frac{\partial^2 M}{\partial x^2} + \rho A \frac{\partial^2 w}{\partial t^2} = 0, \tag{8}$$

where ρ is the material density. Substituting Eq. (6) into Eq. (8) gives the equation of motion for the tapered microbeam as

$$\left[(\lambda + 2\mu) I + \mu\vartheta^2 A\right] \frac{\partial^4 w}{\partial x^4} + \beta \frac{\partial^2 M_T}{\partial x^2} + \rho A \frac{\partial^2 w}{\partial t^2} = 0. \tag{9}$$

In addition, the heat conduction equation in context of the Green-Naghdi's generalized thermoelasticity theory without energy dissipation and without considering the effect of any heat sources is given by

$$K\nabla^2\theta - \frac{\partial}{\partial t}\left[\rho C_E \frac{\partial \theta}{\partial t} - \beta T_0 z \frac{\partial^3 w}{\partial x^2 \partial t}\right] = 0, \tag{10}$$

where C_E represents specific heat per unit mass at constant strain and K denotes thermal conductivity.

3. Solution procedure

The system of Eqs. (9) and (10) governs the transverse vibrations in a thermoelastic tapered micro-machined beam resonators. If we apply the integral operator $\mathcal{L}_1(\cdot)$ to all terms of Eq. (10) and simplifying the outcomes, we obtain

$$\frac{\partial^2 M_T}{\partial x^2} - b\left(\theta\big|_{z=h/2} - \frac{1}{2}\theta\big|_{z=-h/2}\right) + \frac{1}{2}bh\left(\frac{\partial\theta}{\partial z}\bigg|_{z=h/2} + \frac{1}{2}\frac{\partial\theta}{\partial z}\bigg|_{z=-h/2}\right) - \frac{\partial}{\partial t}\left[\zeta\frac{\partial M_T}{\partial t} - \frac{\beta T_0 I}{K}\frac{\partial^3 w}{\partial x^2 \partial t}\right] = 0, \qquad (11)$$

where $\zeta = \rho C_E/K$. For the present tapered microbeam, the upper and lower surfaces are thermally isolated, it follows that

$$\frac{\partial\theta}{\partial z}\bigg|_{z=-h/2} = \frac{\partial\theta}{\partial z}\bigg|_{z=h/2} = 0. \qquad (12)$$

In addition, one can assume that temperature increment has a cubic polynomial variation through-the-thickness of tapered microbeam. So, the above postulate tends to

$$M_T = \frac{h^2 b}{20}\left(\theta\big|_{z=h/2} - \frac{1}{2}\theta\big|_{z=-h/2}\right). \qquad (13)$$

So, at this point Eq. (11) tends to

$$\frac{\partial^2 M_T}{\partial x^2} - \frac{20}{h^2}M_T - \frac{\partial}{\partial t}\left[\zeta\frac{\partial M_T}{\partial t} - \frac{\beta T_0 I}{K}\frac{\partial^3 w}{\partial^2 x \partial t}\right] = 0. \qquad (14)$$

Now, we can improve Eqs. (9), (14) and (6) by introducing the following dimensionless variables:

$$\begin{aligned} x' &= \frac{x}{L}, & \{w', \vartheta'\} &= \frac{1}{h}\{w, \vartheta\}, & t' &= \frac{c}{h}t, \\ M' &= \frac{h}{I\lambda}M, & M'_T &= \frac{\beta h}{I\lambda}M_T, & c^2 &= \frac{\lambda}{\rho}, \end{aligned} \qquad (15)$$

to show that the dimensionless forms of the governing equations as well as the flexural bending moment maybe simplified as (in what follows, the primes are dropping for convenience)

$$A_1\frac{\partial^4 w}{\partial x^4} + A_2\frac{\partial^2 M_T}{\partial x^2} + \frac{\partial^2 w}{\partial t^2} = 0, \qquad (16)$$

$$\frac{\partial^2 M_T}{\partial x^2} - A_3 M_T - \frac{\partial}{\partial t}\left(A_4\frac{\partial M_T}{\partial t} - A_5\frac{\partial^3 w}{\partial x^2 \partial t}\right) = 0, \qquad (17)$$

$$M(xt) = \frac{\vartheta^* h^2}{L^2}\frac{\partial^2 w}{\partial x^2} + M_T, \qquad (18)$$

where

$$A_1 = \frac{\vartheta^* h^4}{12L^4}, \quad A_2 = \frac{h^2}{12L^2}, \quad A_3 = \frac{20L^2}{h^2}, \quad A_4 = \frac{\zeta c^2 L^2}{h^2},$$
$$A_5 = \frac{\beta^2 T_0}{\rho K}, \quad \vartheta^* = 1 + 2\overline{\mu}(1 + 6\vartheta^2), \quad \overline{\mu} = \frac{\mu}{\lambda}. \tag{19}$$

In addition to the heat conditions (thermally isolated) that appear in Eq. (12), the present problem can be completely solved by applying the boundary conditions. The tapered microbeam is subjected to various combination of boundary conditions at the edges $x = 0, 1$. Each edge may be simply-supported (S), clamped (C), or free (F). That is

$$\begin{aligned} \text{S}: \ & w = M = 0, \\ \text{C}: \ & w = \frac{\partial w}{\partial x} = 0, \\ \text{F}: \ & M = \frac{\partial w}{\partial x} = 0. \end{aligned} \tag{20}$$

Now, it is assumed that both the bending moment $M(xt)$ and deflection $w(xt)$ are harmonically changed to discuss vibration characteristics of tapered microbeam. According to Eqs. (18), the thermal bending moment $M_T(xt)$ and bending moment $M(xt)$ have identical behavior. So, the following representations for deflection and thermal bending moment are appropriate in the analysis of the thermal problem (by invoking the dimensionless form):

$$\{w, M_T\} = \sum_{n=1}^{N} \{w_n^*, M_{Tn}^*\} X(\xi_n x) \mathrm{e}^{\mathrm{i}\omega t}, \tag{21}$$

in which w_n^* and M_{Tn}^* represent arbitrary parameters, n denotes a mode number and ω represents eigenfrequency. The function $X(\xi_n x)$ can be deduced for any combination of boundary conditions at side edges of the microbeam ($x = 0, 1$). The forms of $X(\xi_n x)$ for SS, CS, CC, and CF tapered microbeams are expressed as [55]

$$\text{SS}: \sin(\xi_n x) \tag{22}$$

$$\text{CS}: \quad \sin(\xi_n x) - \mathrm{sh}(\xi_n x) - \frac{\mathrm{sh}(\xi_n) + \sin(\xi_n)}{\mathrm{ch}(\xi_n) + \cos(\xi_n)} [\cos(\xi_n x) - \mathrm{ch}(\xi_n x)], \tag{23}$$

$$\text{CC}: \quad \sin(\xi_n x) - \mathrm{sh}(\xi_n x) - \frac{\mathrm{sh}(\xi_n) - \sin(\xi_n)}{\mathrm{ch}(\xi_n) - \cos(\xi_n)} [\cos(\xi_n x) - \mathrm{ch}(\xi_n x)], \tag{24}$$

$$\text{CF}: \quad \sin(\xi_n x) - \mathrm{sh}(\xi_n x) - \frac{\mathrm{sh}(\xi_n) + \sin(\xi_n)}{\mathrm{ch}(\xi_n) + \cos(\xi_n)} [\cos(\xi_n x) - \mathrm{ch}(\xi_n x)], \tag{25}$$

and the corresponding values of ξ_n for tapered microbeams subjected to various boundary conditions are listed in Table 1. Substituting Eq. (21) into Eqs. (16) and (17) gives

$$[A_1\xi_n^4 X(\xi_n x) - \omega^2 X(\xi_n x)]w_n^* + A_2\xi_n^2 X''(\xi_n x)M_{Tn}^* = 0, \tag{26}$$

$$-\omega^2 A_5\xi_n^2 X''(\xi_n x)w_n^* + [\xi_n^2 X''(\xi_n x) - (A_3 - \omega^2 A_4)X(\xi_n x)]M_{Tn}^* = 0. \tag{27}$$

Table 1.

Values of ξ_n according to various boundary conditions [55]

n	BS			
	SS	CS	CC	CF
1	π	3.927	4.730	1.875
2	2π	7.069	7.853	4.694
3	3π	10.210	10.996	7.855
4	4π	13.352	14.137	10.996
$\geqslant 5$	$n\pi$	$\left(n+\frac{1}{4}\right)\pi$	$\left(n+\frac{1}{2}\right)\pi$	$\left(n-\frac{1}{2}\right)\pi$

The nontrivial solution of the above system of equations may be easily given if the two parameters w_n^* and M_{Tn}^* are nonzero. Integrating the above system along the length of the tapered microbeam with respect to x from 0 to 1 one obtains its determinant. The vanishing of this determinant leads to the following vibration frequency equation

$$c_4\omega^4 + c_2\omega^2 + c_0 = 0, \tag{28}$$

where

$$c_4 = A_4\eta_1, \qquad c_2 = \eta_2\xi_n^2 - A_3\eta_1 - \xi_n^4(A_1A_4\eta_1 + A_2A_5\eta_3), \qquad c_0 = (A_3\eta_1 - \eta_2\xi_n^2)A_1\xi_n^4, \tag{29}$$

in which

$$\eta_1 = \int_0^1 [X(\xi_n x)]^2 \mathrm{d}x, \qquad \eta_2 = \int_0^1 X(\xi_n x)X''(\xi_n x)\mathrm{d}x, \qquad \eta_3 = \int_0^1 [X''(\xi_n x)]^2 \mathrm{d}x. \tag{30}$$

It is to be noted that outcomes of above integrals are independent of n since $X(\xi_n x)$ and their derivatives are normalized. Furthermore, some computations will be carrying out to compute the both absolute and real values of the smallest root of the dimensionless eigenfrequency,

$$\Omega = \frac{L^2}{h^2}\sqrt{\frac{\lambda}{12\rho}}\omega. \tag{31}$$

4. Numerical results

Let us consider in this section some numerical examples to put into evidence the influence of couple stress parameter, mode number and the thermoelastic coupling on the minimum eigenfrequency. The present tapered microbeam is made of *Silicon* with material properties given in Table 2 [56]. The relations between the engineering constants E and ν and the corresponding Lame's constants λ and μ are given by

$$\lambda = \frac{E\nu}{(1+\nu)(1-2\nu)}, \qquad \mu = \frac{E}{2(1+\nu)}. \tag{32}$$

Table 2.
Temperature-dependent mechanical and thermal properties of Silicon [56]

T_0 (K)	E (GPa)	ρ (kg/m^3)	ν	K (W/mK)	C_E (J/kg K)	α (1/K)
400	163.1	2327	0.22	105	785	3.253×10^{-6}
293	165.9	2330	0.22	156	713	2.59×10^{-6}
200	166.9	2330	0.22	266	557	1.406×10^{-6}
160	168.5	2330	0.22	375	456	0.689×10^{-6}
120	169.0	2330	0.22	876	823	-0.057×10^{-6}
80	169.2	2330	0.22	1360	188	-0.472×10^{-6}
40	169.3	2330	0.22	3660	44.1	-0.164×10^{-6}

Many values of the dimensionless couple stress coefficient ϑ are imposed. The case of neglecting this coefficient ($\vartheta = 0$) denotes the generalized thermoelasticity theory of the tapered microbeam. The inclusion of the couple stress coefficient, by using additional values of ϑ such that $0 < \vartheta \leqslant 1$, will be referring to the generalized thermoelasticity theory based on modified couple stress analysis.

The effects of couple stress parameter ϑ and mode number n on the vibration frequency of tapered microbeams subjected to various boundary conditions are presented in Table 3. The environmental temperature and the length-to-thickness ratio are kept fixed as $T_0 = 293$ K and $L/h = 20$. The absolute values of the vibration frequencies increase as mode number n increases. However, real values of vibration frequencies may be no longer increasing and vanished with the increasing of the mode number or as L/h increases (see also, Figs 3, 4, 6, 7 and 8). The absolute values of the vibration frequencies due to CF tapered microbeams are the smallest frequencies, while those due to CC tapered microbeams are the largest ones.

Table 3.

Effect of the couple stress parameter ϑ and mode number n on the natural frequencies * Ω of tapered microbeams with various boundary conditions ($L/h = 20$, $T_0 = 293$ K)

ϑ	BC	n = 1	2	3	4	5
0.0	SS	1.08653 (0.71643)	2.26509 (1.15972)	3.85799 (1.12563)	5.52683 (0)	7.37766 (0)
	CS	1.36153 (0.88719)	2.58654 (1.29094)	4.29984 (1.25422)	6.47074 (0)	8.21923 (0)
	CC	1.64481 (1.06608)	2.92145 (1.42985)	4.76520 (1.41212)	7.39143 (0.69424)	9.16943 (0)
	CF	0.64646 (0.45884)	1.63316 (1.05052)	2.92168 (1.43217)	4.76518 (1.41216)	7.39158 (0.69423)
0.3	SS	1.17928 (0.78635)	2.45844 (1.34223)	4.18730 (1.60989)	6.69902 (1.70999)	10.06991 (1.74933)
	CS	1.47774 (0.97575)	2.80732 (1.50398)	4.66687 (1.79405)	7.34775 (1.99635)	10.89020 (2.21380)
	CC	1.78520 (1.17359)	3.17082 (1.67455)	5.17195 (2.00376)	8.02235 (2.31180)	11.73671 (2.68280)
	CF	0.70164 (0.49772)	1.77256 (1.15801)	3.17107 (1.67656)	5.17193 (2.00378)	8.02251 (2.31184)
0.5	SS	1.30437 (0.87959)	2.71920 (1.57373)	4.63144 (2.13310)	7.40957 (2.81718)	11.13801 (3.79291)
	CS	1.63448 (1.09362)	3.10509 (1.77263)	5.16187 (2.37723)	8.12711 (3.16475)	12.04530 (4.25997)
	CC	1.97456 (1.31654)	3.50714 (1.98169)	5.72053 (2.64627)	8.87327 (3.54017)	12.98160 (4.75218)
	CF	0.77606 (0.55019)	1.96057 (1.30074)	3.50742 (1.98343)	5.72051 (2.64628)	8.87345 (3.54024)
1.0	SS	1.64919 (1.13266)	3.43805 (2.16558)	5.85582 (3.31214)	9.36838 (4.93649)	14.08247 (7.17750)
	CS	2.06658 (1.41266)	3.92596 (2.45520)	6.52647 (3.69137)	10.27560 (5.45754)	15.22961 (7.84687)
	CC	2.49655 (1.70300)	4.43430 (2.75836)	7.23282 (4.09845)	11.21902 (6.00821)	16.41344 (8.54533)
	CF	0.98122 (0.69497)	2.47888 (1.68594)	4.43465 (2.75972)	7.23280 (4.09846)	11.21925 (6.00833)

* Results between parentheses are for real frequencies.

The effects of environmental reference temperature T_0 and couple stress parameter ϑ on the fundamental vibration frequencies of the tapered microbeams subjected to various boundary conditions are presented in Table 4. The length-to-thickness ration is kept fixed as $L/h = 10$. For all values of the couple stress parameter ϑ and different boundary conditions, the frequencies increase as T_0 decreases except the cases of $T_0 = 40$ K and $\vartheta \leqslant 0.5$ for SS, CC, and CS tapered

Table 4.
Effect of the couple stress parameter ϑ and the temperature T_0 on the fundamental frequencies * Ω of tapered microbeams with various boundary conditions ($n = 1$, $L/h = 10$)

ϑ	T_0 (K)	BC			
		SS	CS	CC	CF
0.0	400	0.48291 (0.32375)	0.60933 (0.40528)	0.74202 (0.49215)	0.28470 (0.20191)
	293	0.54811 (0.36188)	0.69159 (0.45189)	0.84219 (0.54827)	0.32314 (0.22936)
	200	0.66721 (0.42493)	0.84188 (0.52736)	1.02521 (0.63841)	0.39336 (0.27969)
	160	0.76614 (0.47024)	0.96671 (0.57959)	1.17722 (0.69986)	0.45168 (0.32170)
	120	1.02925 (0.54285)	1.29870 (0.64558)	1.58150 (0.76871)	0.60680 (0.43465)
	80	1.32081 (0.48552)	1.66657 (0.48311)	2.02948 (0.52214)	0.77869 (0.56234)
	40	1.11779 (0)	1.31396 (0)	1.56465 (0)	1.43332 (1.08486)
0.3	400	0.52413 (0.35436)	0.66134 (0.44418)	0.80535 (0.53965)	0.30900 (0.21905)
	293	0.59489 (0.39712)	0.75062 (0.49676)	0.91408 (0.60310)	0.35072 (0.24879)
	200	0.72416 (0.46924)	0.91374 (0.58412)	1.11272 (0.70789)	0.42693 (0.30331)
	160	0.83154 (0.52285)	1.04923 (0.64738)	1.27771 (0.78303)	0.49024 (0.34878)
	120	1.11711 (0.62367)	1.40955 (0.75292)	1.71650 (0.90195)	0.65860 (0.47084)
	80	1.43354 (0.62530)	1.80883 (0.69325)	2.20272 (0.79950)	0.84515 (0.60844)
	40	1.32910 (0)	1.55856 (0)	1.85476 (0)	1.55566 (1.16609)
0.5	400	0.57972 (0.39529)	0.73149 (0.49613)	0.89078 (0.60304)	0.34178 (0.24217)
	293	0.65799 (0.44410)	0.83024 (0.55651)	1.01104 (0.67606)	0.38792 (0.27502)
	200	0.80098 (0.52798)	1.01066 (0.65913)	1.23074 (0.79963)	0.47222 (0.33519)
	160	0.91974 (0.59211)	1.16052 (0.73625)	1.41323 (0.89190)	0.54224 (0.38535)
	120	1.23560 (0.72688)	1.55906 (0.88814)	1.89856 (1.06892)	0.72845 (0.51975)
	80	1.58560 (0.78774)	2.00069 (0.91980)	2.43636 (1.08680)	0.93480 (0.67080)
	40	1.65568 (0)	1.93175 (0)	2.29602 (0)	1.72067 (1.27674)
1.0	400	0.73298 (0.50680)	0.92487 (0.63742)	1.12626 (0.77534)	0.43213 (0.30596)
	293	0.83194 (0.57167)	1.04973 (0.71834)	1.27831 (0.87350)	0.49047 (0.34738)
	200	1.01272 (0.68614)	1.27784 (0.86033)	1.55610 (1.04536)	0.59706 (0.42320)
	160	1.16288 (0.77703)	1.46731 (0.97219)	1.78683 (1.18037)	0.68558 (0.48631)
	120	1.56224 (0.99262)	1.97122 (1.23139)	2.40047 (1.49046)	0.92103 (0.65495)
	80	2.00477 (1.17176)	2.52959 (1.42971)	3.08044 (1.71982)	1.18192 (0.84352)
	40	3.05363 (0)	3.35471 (0)	3.94435 (0)	2.17555 (1.58626)

* Results between parentheses are for real frequencies.

microbeams. In such cases, the real frequencies are vanished. For fixed values of T_0, the eigenfrequencies increase as ϑ increases for all boundary conditions.

Figs 2–7 plot both the absolute and real values of the eigenfrequencies along the length of the tapered microbeam subjected to various boundary conditions. Fig. 2 presents the first-mode fundamental frequency Ω $(n = 1)$ versus L/h for different values of couple stress coefficient ϑ at $T_0 = 293$ K. Both the absolute and real frequency parameters Ω increase directly with the increase of the L/h ratio. The vibration frequencies of tapered microbeam are very sensitive to the variation of couple stress parameter ϑ, especially, at highest values of L/h ratio. Once again, the eigenfrequency increases with the increase of ϑ for all boundary conditions.

Fig. 3 presents third-mode natural frequencies Ω $(n = 3)$ versus L/h for different values of the couple stress coefficient ϑ at $T_0 = 293$ K. It is clear that the

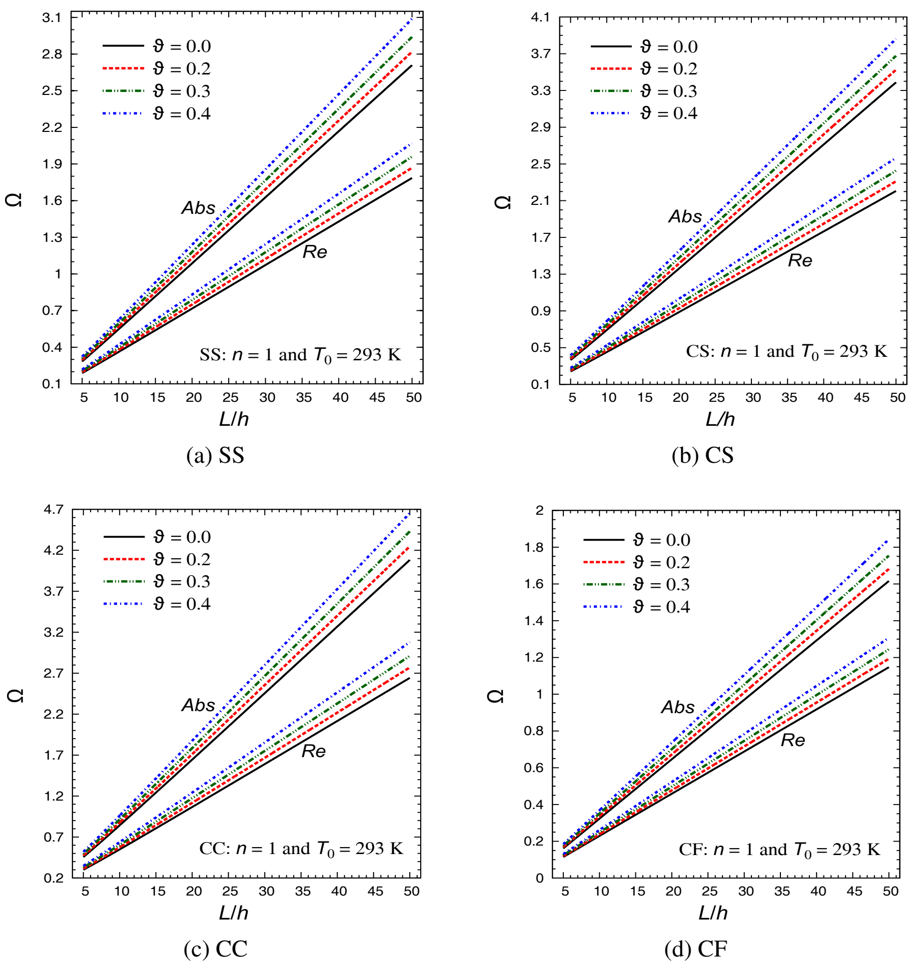

Fig. 2. The first-mode frequency Ω vs. L/h of a tapered microbeam for different values of the couple stress parameter ϑ at $T_0 = 293$ K

natural eigenfrequency Ω increases directly as ϑ increases only for CF tapered microbeams. The same behaviors occur for SS, CC and CS tapered microbeams, especially when $\vartheta > 0.2$. Some dropping points occurred when $\vartheta \leqslant 0.2$ at which the real frequencies tend to zero and the corresponding absolute frequencies may have local maximums. These dropping points occurred for $\vartheta = 0$ and $\vartheta = 0.2$, respectively, when $L/h = 32.8$ and 48.7 for SS microbeam; when $L/h = 29.35$ and 36.85 for CC microbeam; and when $L/h = 30.35$ and 39.95 for CS microbeam.

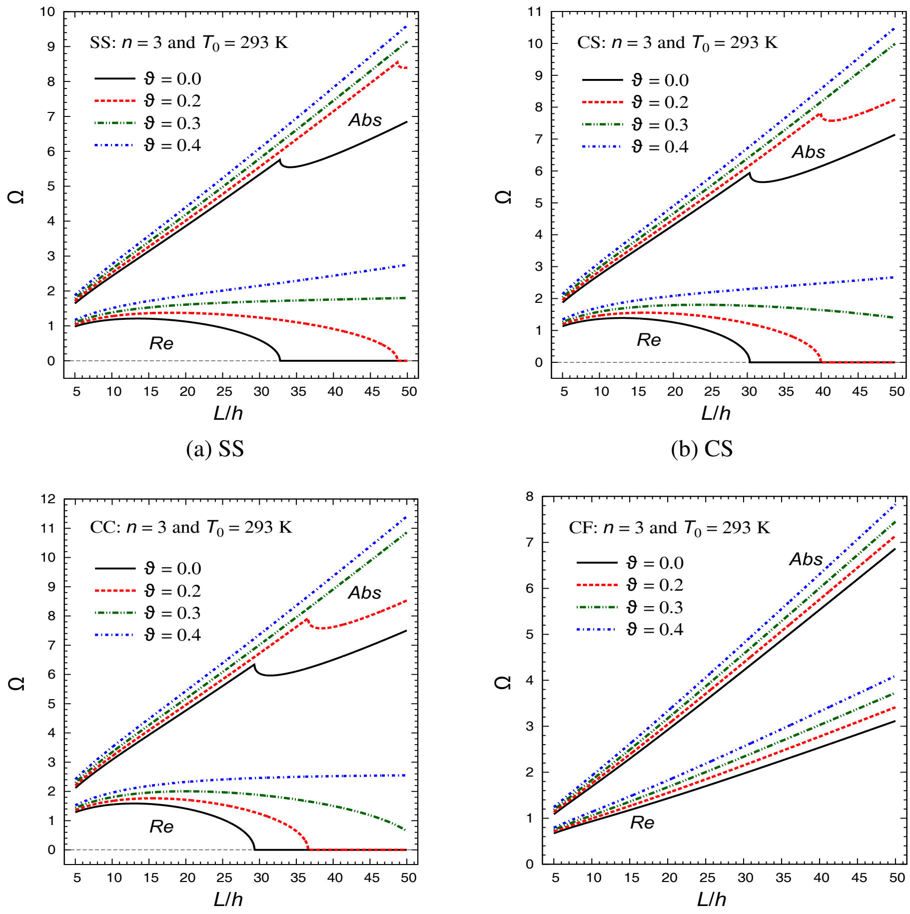

(a) SS (b) CS

(c) CC (d) CF

Fig. 3. The third-mode frequency Ω vs. L/h of a tapered microbeam for different values of the couple stress parameter ϑ at $T_0 = 293$ K

Fig. 4 presents the fifth-mode natural frequencies Ω $(n = 5)$ versus L/h for different values of the couple stress coefficient ϑ at $T_0 = 293$ K. Once again, the natural eigenfrequency Ω increases as ϑ increases with dropping points for tapered

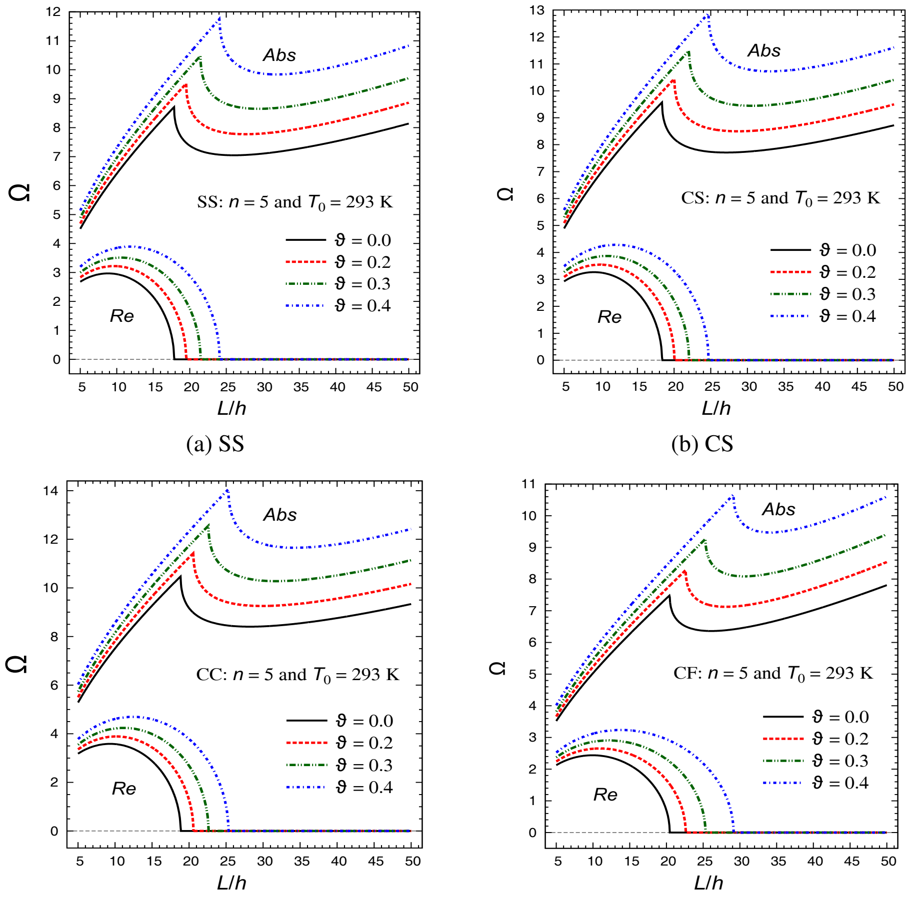

(a) SS (b) CS

(c) CC (d) CF

Fig. 4. The fifth-mode frequency Ω vs. L/h of a tapered microbeam for different values of the couple stress parameter ϑ at $T_0 = 293$ K

microbeams with various boundary conditions. Table 5 presents the positions of the dropping points (the values of L/h) for the fifth-mode vibration frequencies of tapered microbeams according to various boundary conditions at $T_0 = 293$ K.

Table 5.

The positions of the dropping points (the values of L/h) for the fifth-mode vibration frequencies of tapered microbeams according to various boundary conditions ($T_0 = 293$ K)

ϑ	BS			
	SS	CS	CC	CF
0.0	17.90	18.40	18.90	20.45
0.2	19.55	20.05	20.60	22.65
0.3	21.50	22.05	22.65	25.35
0.4	24.10	24.70	25.35	29.15

Figs 5–7 present the fundamental and natural frequencies Ω versus L/h for different values of the couple stress coefficient ϑ at $T_0 = 160$ K. Once again, the first-mode fundamental frequency Ω increases directly as ϑ increases, as shown in Fig. 5.

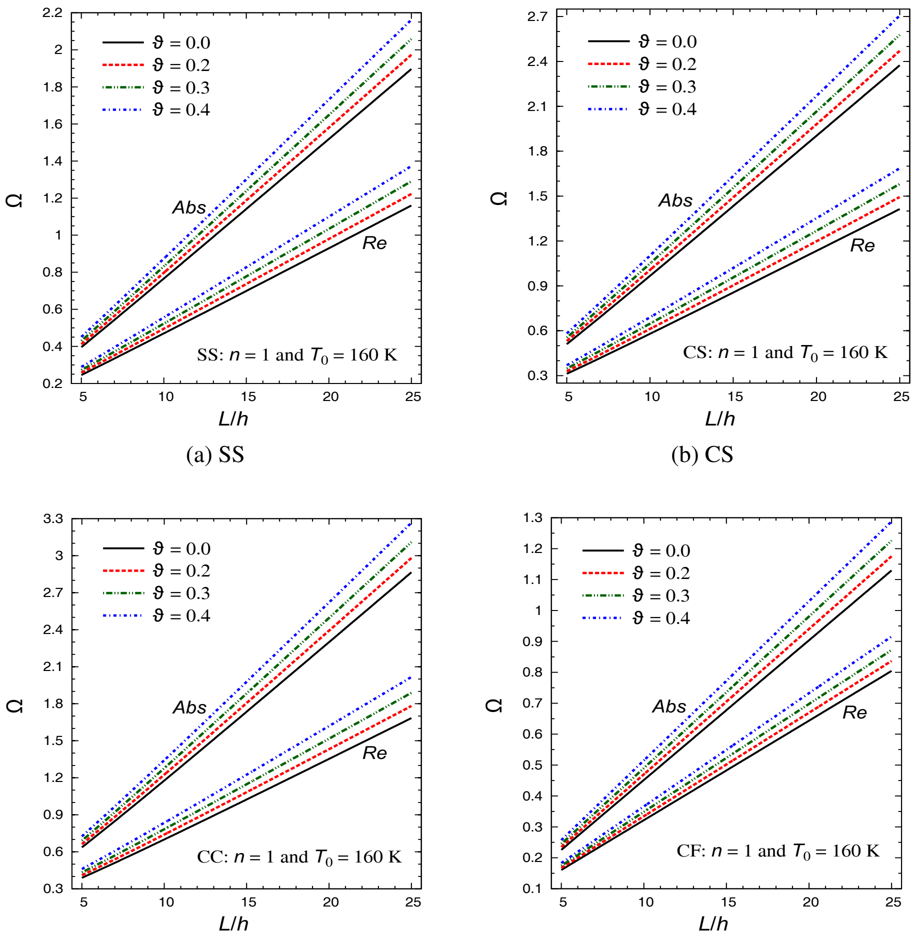

(a) SS (b) CS

(c) CC (d) CF

Fig. 5. The first-mode frequency Ω vs. L/h of a tapered microbeam for different values of the couple stress parameter ϑ at $T_0 = 160$ K

The dropping points maybe appeared for tapered microbeams with various boundary conditions when $n = 3$ and $n = 5$. Table 6 presents the positions of the dropping points (the values of L/h) for third- and fifth-mode vibration frequencies of tapered microbeams according to various boundary conditions at $T_0 = 160$ K. Table 7 presents the positions of the dropping points (the values of L/h) for fifth-mode vibration frequencies of tapered microbeams according to various boundary conditions with $\vartheta = 0.2$.

Table 6.
The positions of the dropping points (the values of L/h) for the vibration frequencies of tapered microbeams according to various boundary conditions (T_0 = 160 K)

n	ϑ	BS			
		SS	CS	CC	CF
3	0.0	9.90	10.25	10.65	20.10
	0.2	10.95	11.35	11.75	—
	0.3	12.25	12.65	13.05	—
	0.4	14.10	14.45	14.85	—
5	0.0	8.95	9.25	9.50	9.80
	0.2	9.75	10.05	10.35	10.70
	0.3	10.60	10.95	11.25	11.70
	0.4	11.75	12.10	12.45	13.00

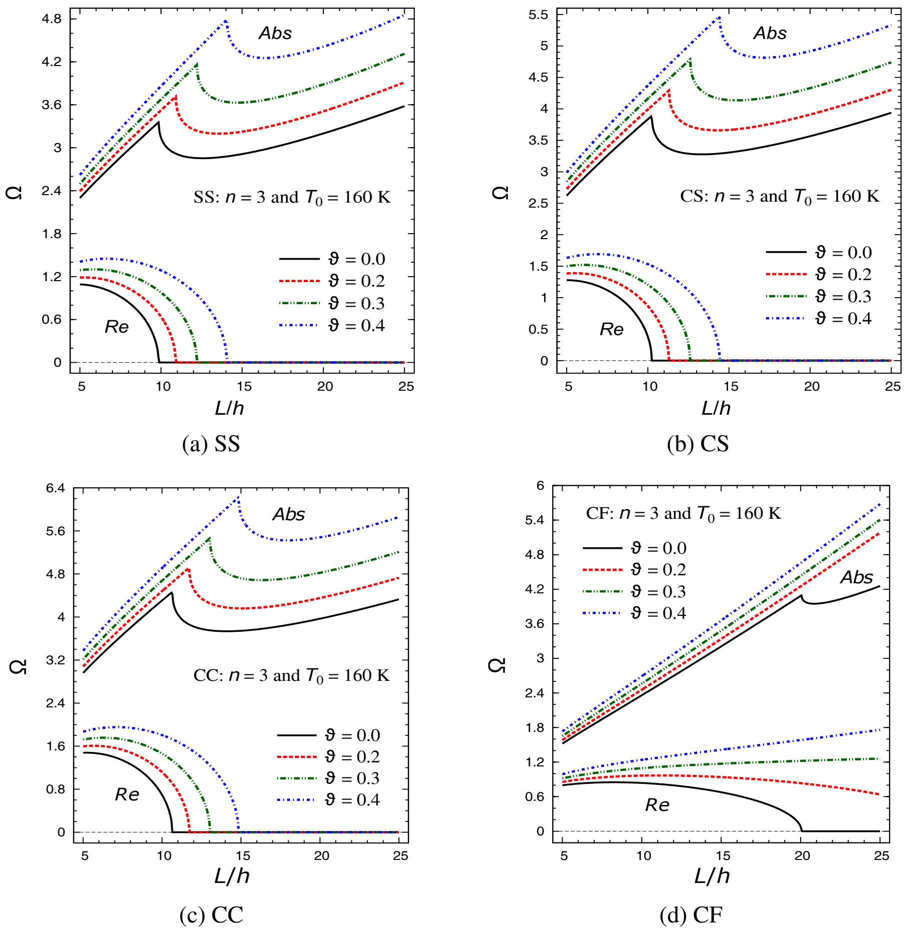

Fig. 6. The third-mode frequency Ω vs. L/h of a tapered microbeam for different values of the couple stress parameter ϑ at T_0 = 160 K

Table 7.
The positions of the dropping points (the values of L/h) for the fifth-mode vibration frequencies of tapered microbeams according to various boundary conditions ($\vartheta = 0.2$)

T_0	BS			
	SS	CS	CC	CF
120	5.40	5.60	5.70	5.80
200	12.85	13.25	13.60	14.30
400	25.75	26.40	27.00	31.75

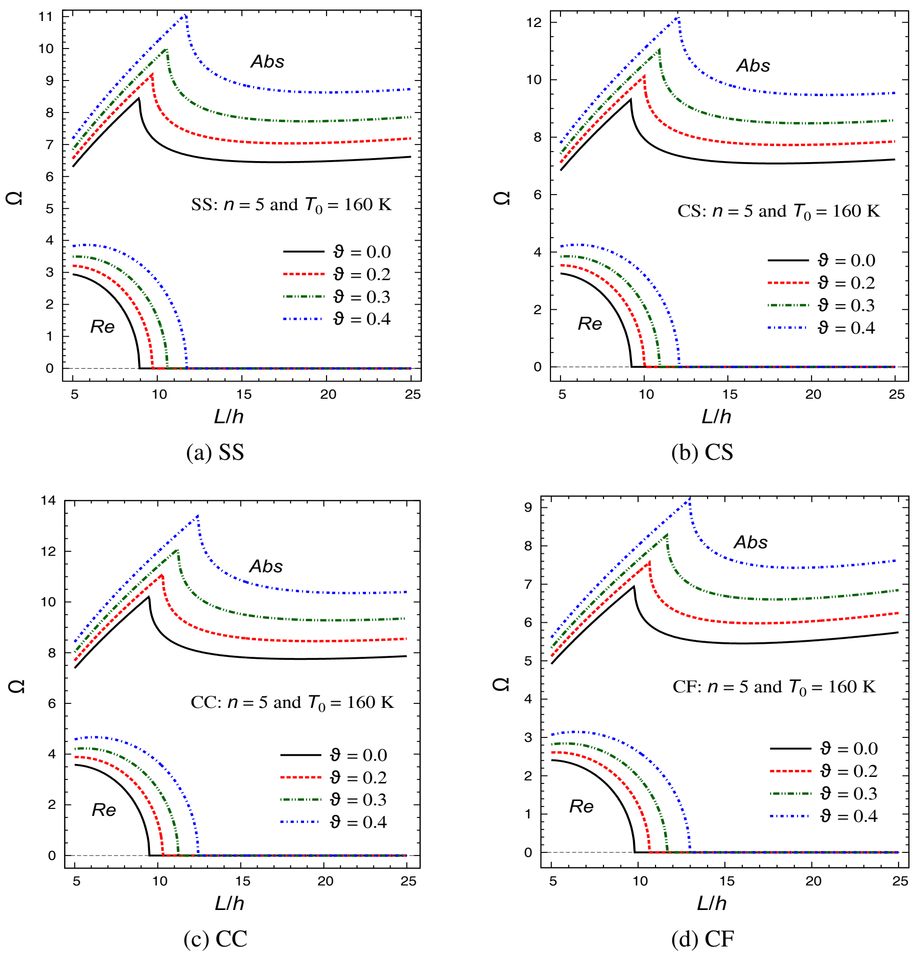

Fig. 7. The fifth-mode frequency Ω vs. L/h of a tapered microbeam for different values of the couple stress parameter ϑ at $T_0 = 160$ K

Finally, Fig. 8 presents the fifth-mode natural frequency Ω ($n = 5$) versus L/h of tapered microbeams for different values of the reference temperature T_0 with $\vartheta = 0.2$. The real frequencies are vanished for all tapered microbeams when

$T_0 = 40$ K. The dropping points occurred at three different positions according to the value of the reference temperature. Before and at the neighborhood of the first dropping point ($T_0 = 120$ K), the absolute frequencies increase as T_0 decreases. However, at the neighborhood and after the fourth dropping point ($T_0 = 400$ K) the absolute frequencies increase as T_0 increases. It is interesting to see that the maximum value of the real frequency is the same for the reference temperatures $T_0 = 200$ K and $T_0 = 400$ K. Also, the dropping points represent the maximum values of the absolute natural frequencies.

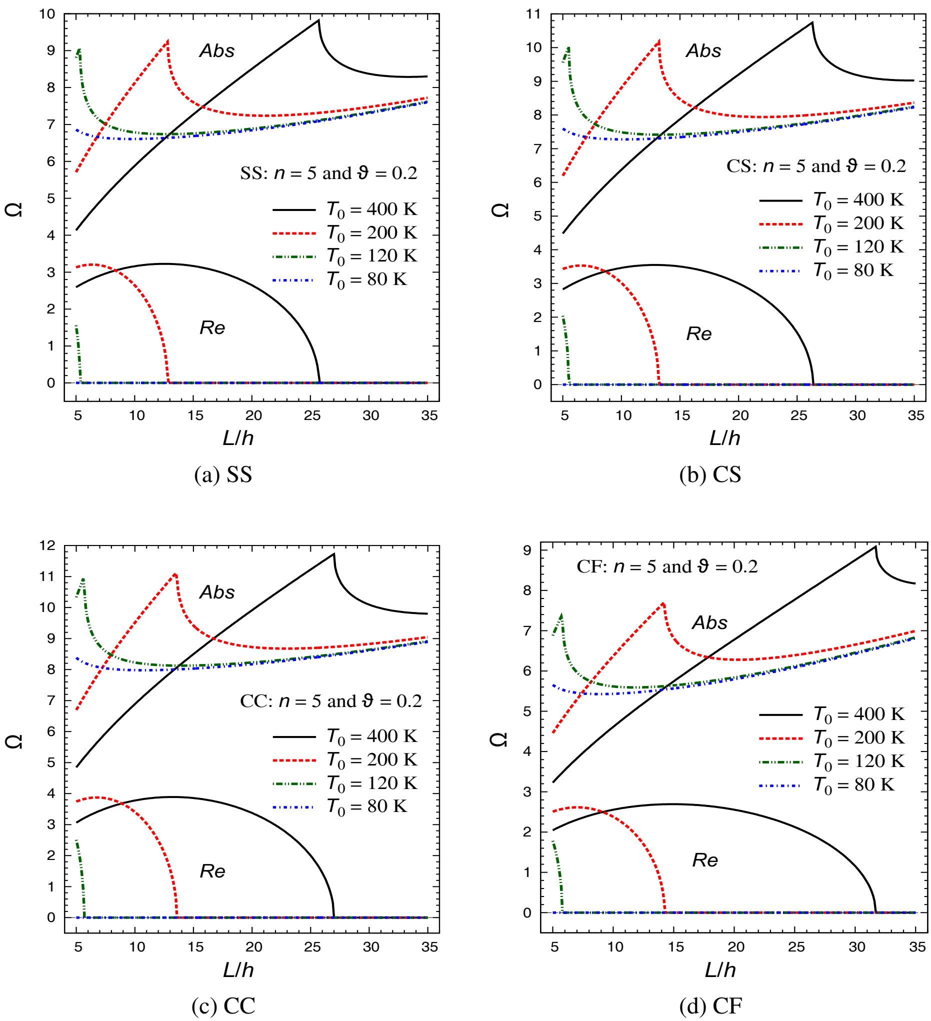

(a) SS (b) CS

(c) CC (d) CF

Fig. 8. The fifth-mode frequency Ω vs. L/h of a tapered microbeam for different temperatures with $\vartheta = 0.2$

5. Conclusions

This article presents numerical results for fundamental and natural frequencies of tapered microbeams to serve as benchmarks for future comparisons with other investigators. The real and absolute eigenfrequencies are presented for thermally-insulated tapered microbeams under a combination of various boundary conditions. The modified couple stress thermoelastic vibrations of tapered microbeams with variable reference temperature are presented. The employed non-classical continuum theory contains one material length-scale parameter, which can capture the small-scale effect. Green-Naghdi's generalized theory of thermoelasticity without energy dissipation is appropriated to discuss such problem. The influences of length-scale parameter on vibration behaviors of microbeams are discussed in detail for clamped, free, and simply-supported edge conditions. It is clear that the couple stress coefficient plays a significant role in fundamental and natural eigenfrequency behaviors. The temperature invariant has also significant effects on thermomechanical dynamical behaviors of tapered microbeams. The absolute and real vibration frequencies of the tapered microbeams with various boundary conditions are strongly dependent on the couple stress parameter. The results of standard (without couple stress) thermoelasticity theory can be obtained as a limiting case of the present study.

Manuscript received by Editorial Board, May 19, 2017;
final version, December 13, 2017.

References

[1] E. Cosserat and F. Cosserat. Theory of Deformable Bodies. Herman et Fils, Paris (1909).

[2] R.A. Toupin. Elastic materials with couple-stresses. *Archive for Rational Mechanics and Analysis*, 11(1):385–414, 1962. doi: 10.1007/BF00253945.

[3] R.D. Mindlin and H.F. Tiersten. Effects of couple-stresses in linear elasticity. *Archive for Rational Mechanics and Analysis*, 11:415–448, 1962. doi: 10.1007/BF00253946.

[4] W.T. Koiter. Couple-stresses in the theory of elasticity: I and II. Proc. K. Ned. Akad. Wet.-Amsterdam B, 67:17–44, 1964.

[5] G. Tiwari. Effect of couple-stresses in a semi-infinite elastic medium due to impulsive twist over the surface. *Pure and Applied Geophysics*, 91(1):71–75, 1971.

[6] M. Braun. Linear Elasticity with Couple Stresses. In J.-F. Ganghoffer and F. Pastrone, editors, *Mechanics of Microstructured Solids 2*. Volume 50 of the series Lecture Notes in Applied and Computational Mechanics, pages 1–8, 2010. doi: 10.1007/978-3-642-05171-5_1.

[7] F. Yang, A.C.M. Chong, D.C.C. Lam and P. Tong. Couple stress based strain gradient theory for elasticity. *International Journal of Solids and Structures*, 39(10):2731–2743, 2002. doi: 10.1016/S0020-7683(02)00152-X.

[8] S.K. Park and X.-L. Gao. Bernoulli-Euler beam model based on a modified couple stress theory. *Journal of Micromechanics and Microengineering*, 16(11):2355–2359, 2006. doi: 10.1088/0960-1317/16/11/015.

[9] S.K. Park and X.-L. Gao. Variational formulation of a modified couple stress theory and its application to a simple shear problem. *Zeitschrift für angewandte Mathematik und Physik*, 59(5):904–917, 2008. doi: 10.1007/s00033-006-6073-8.

[10] H.M. Ma, X.-L. Gao and J.N. Reddy. A microstructure-dependent Timoshenko beam model based on a modified couple stress theory. *Journal of the Mechanics and Physics of Solids*, 56(12):3379–3391, 2008. doi: 10.1016/j.jmps.2008.09.007.

[11] H.M. Ma, X.-L. Gao and J.N. Reddy. A non-classical Mindlin plate model based on a modified couple stress theory. *Acta Mechanica*, 220(1-4):217–235, 2011. doi: 10.1007/s00707-011-0480-4.

[12] G.C. Tsiatas. A new Kirchhoff plate model based on a modified couple stress theory. *International Journal of Solids and Structures*, 46(13):2757–2764, 2009. doi: 10.1016/j.ijsolstr.2009.03.004.

[13] L. Yin, Q. Qian, L. Wang and W. Xia. Vibration analysis of microscale plates based on modified couple stress theory. *Acta Mechanica Solida Sinica*, 23(5):386–393, 2010. doi: 10.1016/S0894-9166(10)60040-7.

[14] Y. Fu and J. Zhang. Modeling and analysis of microtubules based on a modified couple stress theory. *Physica E: Low-dimensional Systems and Nanostructures*, 42(5):1741–1745, 2010. doi: 10.1016/j.physe.2010.01.033.

[15] U. Güven. The investigation of the nonlocal longitudinal stress waves with modified couple stress theory. *Acta Mechanica*, 221(3-4):321–325, 2011. doi: 10.1007/s00707-011-0500-4.

[16] J.N. Reddy and A. Arbind. Bending relationships between the modified couple stress-based functionally graded Timoshenko beams and homogeneous Bernoulli–Euler beams. *Annals of Solid and Structural Mechanics*, 3(1-2):15–26, 2012. doi: 10.1007/s12356-012-0026-z.

[17] W. Chen and X. Li. Size-dependent free vibration analysis of composite laminated Timoshenko beam based on new modified couple stress theory. *Archive of Applied Mechanics*, 83(3):431–444, 2013. doi: 10.1007/s00419-012-0689-2.

[18] X.-L. Gao, J.X. Huang and J.N. Reddy. A non-classical third-order shear deformation plate model based on a modified couple stress theory. *Acta Mechanica*, 224(11):2699–2718, 2013. doi: 10.1007/s00707-013-0880-8.

[19] Y-G. Wang, W-H. Lin and C-L. Zhou. Nonlinear bending of size-dependent circular microplates based on the modified couple stress theory. *Archive of Applied Mechanics*, 84(3):391–400, 2014. doi: 10.1007/s00419-013-0807-9.

[20] W. Chen and X. Li. A new modified couple stress theory for anisotropic elasticity and microscale laminated Kirchhoff plate model. *Archive of Applied Mechanics*, 84(3):323–341, 2014. doi: 10.1007/s00419-013-0802-1.

[21] H. Darijani and A.H. Shahdadi. A new shear deformation model with modified couple stress theory for microplates. *Acta Mechanica*, 226(8):2773–2788, 2015. doi: 10.1007/s00707-015-1338-y.

[22] H. Zeighampour and Y.T. Beni. A shear deformable cylindrical shell model based on couple stress theory. *Archive of Applied Mechanics*, 85(4):539–553, 2015. doi: 10.1007/s00419-014-0929-8.

[23] A.R. Setoodeh, M. Rezaei, and M.R. Zendehdel Shahri. Linear and nonlinear torsional free vibration of functionally graded micro/nano-tubes based on modified couple stress theory. *Applied Mathematics and Mechanics*, 37(6):725–740, 2016. doi: 10.1007/s10483-016-2085-6.

[24] R. Sourki and S.A.H. Hoseini. Free vibration analysis of size-dependent cracked microbeam based on the modified couple stress theory. *Applied Physics A*, 122(413):1–11, 2016. doi: 10.1007/s00339-016-9961-6.

[25] M. Asghari, M.H. Kahrobaiyan, M. Rahaeifard, and M.T. Ahmadian. Investigation of the size effects in Timoshenko beams based on the couple stress theory. *Archive of Applied Mechanics*, 81(7):863–874, 2011. doi: 10.1007/s00419-010-0452-5.

[26] U. Güven. Two mode Mindlin–Herrmann rod solution based on modified couple stress theory. *ZAMM - Zeitschrift für Angewandte Mathematik und Mechanik*, 94(12):1011–1016, 2014. doi: 10.1002/zamm.201300066.

[27] G.C. Tsiatas and A.J. Yiotis. Size effect on the static, dynamic and buckling analysis of orthotropic Kirchhoff-type skew micro-plates based on a modified couple stress theory: comparison with the nonlocal elasticity theory. *Acta Mechanica*, 226:1267–1281, 2015. doi: 10.1007/s00707-014-1249-3.

[28] R. Ansari, M.A. Ashrafi, and A. Arjangpay. An exact solution for vibrations of postbuckled microscale beams based on the modified couple stress theory. *Applied Mathematical Modelling*, 39(10–11):3050–3062, 2015. doi: 10.1016/j.apm.2014.11.029.

[29] Y.S. Li and E. Pan. Static bending and free vibration of a functionally graded piezoelectric microplate based on the modified couple-stress theory. *International Journal of Engineering Science*, 97:40–59, 2015. doi: 10.1016/j.ijengsci.2015.08.009.

[30] Y.T. Beni, F. Mehralian, and H. Razavi. Free vibration analysis of size-dependent shear deformable functionally graded cylindrical shell on the basis of modified couple stress theory. *Composite Structures*, 120:65–78, 2015. doi: 10.1016/j.compstruct.2014.09.065.

[31] H. Salehipour, H. Nahvi, and A.R. Shahidi. Exact closed-form free vibration analysis for functionally graded micro/nano plates based on modified couple stress and three-dimensional elasticity theories. *Composite Structures*, 124:283–291, 2015. doi: 10.1016/j.compstruct.2015.01.015.

[32] J. Lou and L. He. Closed-form solutions for nonlinear bending and free vibration of functionally graded microplates based on the modified couple stress theory. *Composite Structures*, 131:810–820, 2015. doi: 10.1016/j.compstruct.2015.06.031.

[33] J. Lou, L. He, and J. Du. A unified higher order plate theory for functionally graded microplates based on the modified couple stress theory. *Composite Structures*, 133:1036–1047, 2015. doi: 10.1016/j.compstruct.2015.08.009.

[34] M. Ghadiri and N. Shafiei. Vibration analysis of rotating functionally graded Timoshenko microbeam based on modified couple stress theory under different temperature distributions. *Acta Astronautica*, 121:221–240, 2016. doi: 10.1016/j.actaastro.2016.01.003.

[35] E.K. Kakhki, S.M. Hosseini, and M. Tahani. An analytical solution for thermoelastic damping in a micro-beam based on generalized theory of thermoelasticity and modified couple stress theory. *Applied Mathematical Modelling*, 40(4):3164–3174, 2016. doi: 10.1016/j.apm.2015.10.019.

[36] R. Kumar, S. Devi, and V. Sharma. A problem of thick circular plate in modified couple stress thermoelastic diffusion with phase-lags. *Multidiscipline Modeling in Materials and Structures*, 12(3):478–494, 2016. doi: 10.1108/MMMS-09-2015-0054.

[37] R. Kumar and S. Devi. Effect of phase-lag on thick circular plate with heat sources in modified couple stress thermoelastic medium. *Journal of Mechanics*, 32(6):665–671, 2016. doi: 10.1017/jmech.2016.25.

[38] R. Kumar and S. Devi. Thermoelastic beam in modified couple stress thermoelasticity induced by laser pulse. *Computers and Concrete*, 19(6):701–710, 2017. doi: 10.12989/cac.2017.19.6.701.

[39] W. Nowacki. Couple-Stresses in the Theory of Thermoelasticity. In H. Parkus et al., editors, *Irreversible Aspects of Continuum Mechanics and Transfer of Physical Characteristics in Moving Fluids*, Part of the series IUTAM Symposia, pages 259–278, 1968. doi: 10.1007/978-3-7091-5581-3_17.

[40] G. Rezazadeh, A. S. Vahdat, S. Tayefeh-rezaei and C. Cetinkaya. Thermoelastic damping in a micro-beam resonator using modified couple stress theory. *Acta Mechanica*, 223(6):1137–1152, 2012. doi: 10.1007/s00707-012-0622-3.

[41] E. Taati, M. M. Najafabadi and H. B. Tabrizi. Size-dependent generalized thermoelasticity model for Timoshenko microbeams. *Acta Mechanica*, 225(7):1823–1842, 2014. doi: 10.1007/s00707-013-1027-7.

[42] R. Kumar, K. Kumar and R.C. Nautiyal. Plane waves and fundamental solution in a couple stress generalized thermoelastic solid. *Afrika Matematika*, 25(3):591–603, 2014. doi: 10.1007/s13370-013-0136-8.

[43] Z-Y. Zhong, W-M. Zhang, G. Meng, and M-Y. Wang. Thermoelastic damping in the size-dependent microplate resonators based on modified couple stress theory. *Journal of Microelectromechanical Systems*, 24(2):431–445, 2015. doi: 10.1109/JMEMS.2014.2332757.

[44] R. Kumar. Response of thermoelastic beam due to thermal source in modified couple stress theory. *CMST*, 22(2):95–101, 2016. doi: 10.12921/cmst.2016.22.02.004.

[45] A.M. Zenkour. Elastic behaviour of an orthotropic beam/one-dimensional plate of uniform and variable thickness. *Journal of Engineering Mathematics*, 44(4):331–344, 2002. doi: 10.1023/A:1021255410184.

[46] A.M. Zenkour. Thermoelastic solutions for annular disks with arbitrary variable thickness. *Structural Engineering and Mechanics*, 24(5):515–528, 2006. doi: 10.12989/sem.2006.24.5.515.

[47] A.M. Zenkour. Stresses in cross-ply laminated circular cylinders of axially variable thickness. *Acta Mechanica*, 187(1–4):85–102, 2006. doi: 10.1007/s00707-006-0356-1.

[48] A.M. Zenkour, M.N.M. Allam, and D.S. Mashat. Linear bending analysis of inhomogeneous variable-thickness orthotropic plates under various boundary conditions. *International Journal of Computational Methods*, 4(3):417–438, 2007. doi: 10.1142/S021987620700128X.

[49] M.N.M. Allam, A.M. Zenkour, and E.R. Elazab. The rotating inhomogeneous elastic cylinders of variable-thickness and density. *Applied Mathematics & Information Sciences*, 2(3):237–257, 2008.

[50] A.M. Zenkour and D.S. Mashat. Exact solutions for variable-thickness inhomogeneous elastic plates under various boundary conditions. *Meccanica*, 44(4):433–447, 2009. doi: 10.1007/s11012-008-9181-z.

[51] A.M. Zenkour. Stresses in a rotating variable-thickness heterogeneous viscoelastic composite cylinder. *Applied Mathematics and Mechanics – Engl. Ed.*, 32(4):1–14, 2011. doi: 10.1007/s10483-011-1434-9.

[52] D. Grover. Viscothermoelastic vibrations in micro-scale beam resonators with linearly varying thickness. *Canadian Journal of Physics*, 90(5):487–496, 2012. doi: 10.1139/p2012-044.

[53] B. Akgöz and Ö. Civalek. Free vibration analysis of axially functionally graded tapered Bernoulli–Euler microbeams based on the modified couple stress theory. *Composite Structures*, 98:314–322, 2013. doi: 10.1016/j.compstruct.2012.11.020.

[54] D.S. Mashat and A.M. Zenkour. Hygrothermal bending analysis of a sector-shaped annular plate with variable radial thickness. *Composite Structures*, 113:446–458, 2014. doi: 10.1016/j.compstruct.2014.03.044.

[55] L.V. Kantorovich and V.I. Krylov. *Approximate methods of higher analysis*. Moscow, Fismatgiz, 1962.

[56] Y. Sun and M. Saka. Thermoelastic damping in micro-scale circular plate resonators. *Journal of Sound and Vibrations*, 329(3):328–337, 2010. doi: 10.1016/j.jsv.2009.09.014.